AUTHOR QUERY FORM

ELSEVIER	**Journal: GEOMOR** **Article Number: 3424**	**Please e-mail or fax your responses and any corrections to:** **E-mail: corrections.esch@elsevier.spitech.com** **Fax: +1 619 699 6721**

Dear Author,

Any queries or remarks that have arisen during the processing of your manuscript are listed below and highlighted by flags in the proof. Please check your proof carefully and mark all corrections at the appropriate place in the proof (e.g., by using on-screen annotation in the PDF file) or compile them in a separate list.

For correction or revision of any artwork, please consult http://www.elsevier.com/artworkinstructions.

No queries have arisen during the processing of your article.

Thank you for your assistance.

Geomorphology xxx (2010) xxx–xxx

Contents lists available at ScienceDirect

Geomorphology

journal homepage: www.elsevier.com/locate/geomorph

Basin and river profile morphometry: A new index with a high potential for relative dating of tectonic uplift

A. Demoulin *

Fund for Scientific Research (FSR-FNRS), Belgium
Dept. of Physical Geography and Quaternary, Univ. of Liège, Belgium

ARTICLE INFO

Article history:
Received 24 June 2010
Received in revised form 22 October 2010
Accepted 25 October 2010
Available online xxxx

Keywords:
Drainage basin morphometry
Timing of uplift
Drainage network response
Western Rhenish shield
R_1 index
S_r index

ABSTRACT

Geomorphometry may be a powerful tool to describe the characteristics of the landscape's response to tectonic signals, but the meaning of morphometric indices is often obscured by the interplay between the many variables controlling the geomorphological evolution. Moreover, although the so-called hypsometric integral refers to the basin scale, most indices are generally derived from the river long profiles and thus focus mainly on the short-term response of a drainage network to base level change, providing limited information in regions of older and/or moderate uplift. Here, using the Rhenish shield (western Europe), an area of moderate Quaternary uplift, as a test case, I attempt to build an index yielding a comprehensive view of the stage attained by the landscape's response and, indirectly, an evaluation of the timing of the triggering base level change. This index, called R_1, is a ratio of differences between the three integrals linked respectively to the classical basin's hypsometric curve, to the main river's long profile, and at the intermediate level, to a 'drainage network's hypsometric curve'. While its ratio form minimizes the lithological effect on R_1, this index is strongly correlated with basin size (regional correlation coefficients are in the range 0.88–0.93), reflecting the way an erosion wave propagates from the outlet of a basin toward its headwaters. Therefore, it is not directly usable as a proxy for relative uplift age. However, one can show that the relation between R_1 and basin size is theoretically expected to change with time. Following uplift, the slope S_r of the linear relation $R_1 = f(\ln A)$ first increases rapidly but briefly, then it gradually diminishes over several million years. This is fully confirmed by the analysis of R_1 and S_r in the study area. Once its initial increase is completed (assumedly in a few ten thousand years), S_r appears to be a reliable indicator of relative uplift (or any other cause of base level lowering) age.

1. Introduction

Dealing with relief generation and evolution at regional or larger scale, geomorphometry may be a powerful tool provided appropriate variables are considered. Several geomorphometric indices characteristic of individual river profiles and of the drainage basin as a whole have been formulated to describe the morphogenic stages of the landscape response to a pulse of tectonic uplift (or a change in relative base level), but they all proved to be effective only in particular settings marked by highly specific conditions. Beyond consideration of its asymmetry, which is rather concerned with surface tilting, the drainage basin is usually described by its hypsometric integral (denoted $\int H_b$ in this paper), a volumetric index first proposed by Strahler (1952). The $\int H_b$ is the integral of the cumulative distribution of relative altitude within a catchment and, sometimes with the related statistics of the hypsometric curve (Harlin, 1978), it has been used to provide a rough evaluation of the stage attained in the long-term evolution of a landscape (Strahler, 1957). Although the spatial variations of $\int H_b$ may be helpful to demonstrate uplift propagation across a region of homogeneous lithology (Delcaillau et al., 1998), they much more often show no clear relation to differential tectonics (Pérez-Peña et al., 2009; Sougnez and Vanacker, 2009). After many others (e.g., Lifton and Chase, 1992; Hurtrez and Lucazeau, 1999), Cohen et al. (2008) also showed that lithology exerts a main control on $\int H_b$, thus strongly interfering with the latter's response to a possible tectonic signal. Furthermore, $\int H_b$ has also been found to correlate with basin size in some cases (Hurtrez et al., 1999; Chen et al., 2003) and not in other cases (Walcott and Summerfield, 2008). In summary, the $\int H_b$ index is generally unable to detect variations in uplift age at a timescale lower than several 10^6 years.

As for river long profiles, their analysis has given rise to an abundant literature that proposed a number of morphometric indices, a review of which is beyond the scope of this article. Among such indices quantitatively describing the profile shape are, e.g., the stream gradient index, either in its *SL* form (Hack, 1957, 1973) or its generalized *DS* form (Goldrick and Bishop, 2007), the steepness *k* and

* Corresponding author. Dept. of Physical Geography and Quaternary, Univ. of Liège, Belgium. Tel.: +32 4366 56 60; fax: +32 4366 57 22.
E-mail address: ademoulin@ulg.ac.be.

0169-555X/$ – see front matter © 2010 Published by Elsevier B.V.
doi:10.1016/j.geomorph.2010.10.033

concavity θ of the slope–area relationship (Willgoose, 1994), the stream concavity indices H_{max} and E_q (Demoulin, 1998), or simply the mean profile gradient of rivers of particular Strahler's orders (Merritts and Vincent, 1989; Merritts and Hesterberg, 1994). Characteristically, as opposed to the catchment's hypsometric integral, they all refer to the landscape's shortest-term response, not exceeding a few 10^4 years, at maximum a few 10^5 years for the first-order streams. Moreover, another common, though diversely marked, weakness remains the persisting difficulty of distinguishing between especially lithological and tectonic signals embedded in their variations either along a single profile or between profiles.

The morphometric analysis of drainage networks has concentrated on their two-dimensional characteristics (hierarchy, density, confluence ratio) and was generally not aimed at revealing tectonic information. By contrast, other indices were devised to be used explicitly in tectonic environments like, e.g., the ratio of valley floor width to valley height that Bull and McFadden (1977) applied to valleys crossing mountain fronts in order to evaluate the latter's uplift rate.

The objective of this paper is to build composite morphometric indices that would be both sensitive to tectonic influences and as universal as possible, and to explore their ability to get rid of the noise of lithological origin and to date (at least relatively) the tectonic forcing of landscape rejuvenation in regions of moderate relief. In other words, I am searching for an index capable of extracting a time signal independent of spatial variations of the process celerity resulting from, e.g., lithology, climate, or sediment load. For that purpose, I will attempt to take advantage of the volumetric information delivered by the drainage network considered as a middle-term between trunk stream and catchment. Moreover, aiming to derive an index usable in most settings, I deliberately rely on an almost universally available, though of poor resolution, data source, i.e., the SRTM 3″ digital elevation model in its 'filled' version 2.

2. Study area

As a test area, I selected the western half of the Paleozoic Rhenish shield (WRS), west of the Rhine valley, and its southern confines up to the Palatinate Mountains. This represents a moderately uplifted area of ~240 × 170 km^2 encompassing the Ardennes and Eifel to the north, the Hunsrück, the Permo-Carboniferous Saar-Nahe basin, and the northern part of the Palatinate Mountains (Fig. 1). The WRS is drained by the thoroughgoing Meuse, Rhine, and Mosel Rivers and their tributaries.

With maximum altitudes of 880 m in the Taunus and 816 m in the Hunsrück, the (W)RS is one of the large Variscan massifs located in the northern foreland of the Alpine arc. Straddling the European Cenozoic rift system, it separates the latter's segments of the Upper Rhine graben to the south and the Lower Rhine Embayment to the north (Fig. 1). In between, the NW-striking deep furrow of the Rhine valley cuts across the massif, going also through the small Neuwied basin where the Rhine river receives two main tributaries, the Mosel from the west and the Lahn from the east. The southern edge of the WRS corresponds to the major Hunsrück-Taunus border fault that separates it from the Saar-Nahe basin, a molasse basin within the Variscan orogen. The Ardennes massif represents a western annex to the RS. Chiefly drained by rivers of the Meuse catchment, it extends between the Paris basin to the south and the Cenozoic Anglo-Belgian basin to the north. Except for limited outcrops of Cambrian quartzites in the Caledonian massifs of the Ardennes and of Devonian limestones and Triasic sandstones in the Eifel, the WRS is overwhelmingly slaty. By contrast, the fluviolacustrine, coal-bearing sediments of the Saar-Nahe basin alternate siliciclastics of varying grain size, from conglomerates to pelitic rocks, while the northern Palatinate Mountains display only Triasic sandstones. Scattered volcanics of Permian to Quaternary age are also present in the Eifel and the Saar-Nahe area. However, the bedrock erodibility may be globally regarded as fairly uniform within the study area.

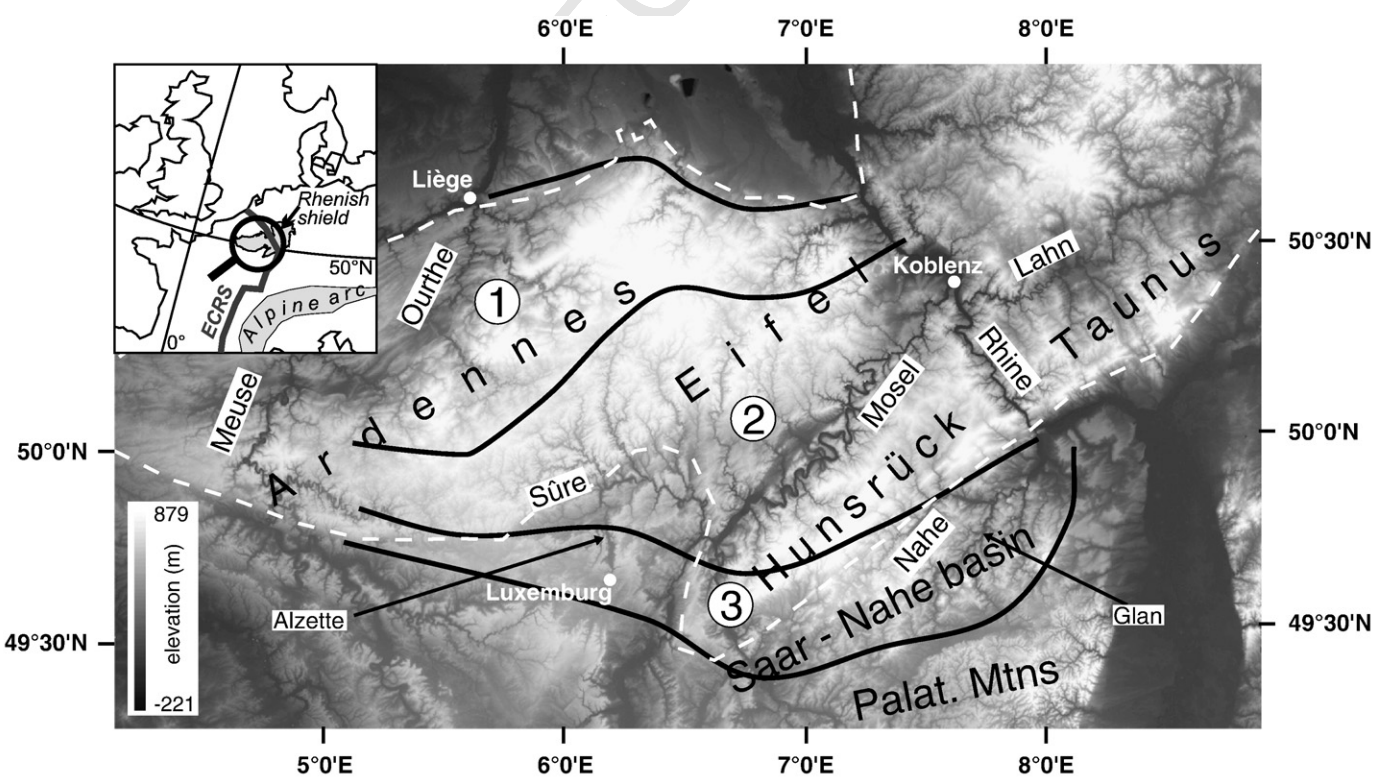

Fig. 1. Digital elevation model of the study area locating the three subareas of different uplift age (younger from 3 to 1) and the rivers named in the text (the elevation scale extends down to minus 221 m because of the presence of the opencast mine of Hambach in the north of the map). The inset shows location within northwest Europe.

The deformation of well-reconstructed Tertiary planation surfaces and their present-day elevations demonstrate that the WRS underwent rock uplift of ~450 m, locally even more than 500 m, since the Oligocene, seemingly mainly in response to far-field stresses (Alpine push and Atlantic ridge opening) (Ziegler and Dèzes, 2007; Demoulin and Hallot, 2009). The seas that episodically encroached on its margins during the Cenozoic and the narrow vertical range occupied by the stepped planation surfaces that developed in these times, however, testify to a low-lying continental area with altitudes not exceeding 200–250 m and only minor vertical motion of the WRS until the Pliocene. By contrast, the deep incision of the valleys in the massif bears witness to a Quaternary acceleration of the uplift. Fluvial terrace studies in the Rhine, Meuse, and Mosel valleys and in their tributaries suggest that the uplift rate increased a first time at the Pliocene–Pleistocene transition and again toward the beginning of the middle Pleistocene to reach maximum values of ~0.5 mm/y in NE Ardennes and Eifel between 0.73 and 0.4 Ma before coming back to tectonic quiescence in recent times (Van den Berg, 1996; Van Balen et al., 2000; Demoulin et al., 2009). As a consequence of this two-step increase in incision rate, a typical valley cross section in the RS opposes a narrow, steep-sided young valley nested into a broader older valley with gently sloping valleysides carved into the Tertiary paleotopography. Dated ~0.73 Ma (Van Balen et al., 2000; Boenigk and Frechen, 2006), the lower level of the so-called Main Terrace complex clearly separates the two units and marks the beginning of the middle Pleistocene incision episode.

A recent reappraisal of the WRS uplift since 0.73 Ma reduced its maximum amount from 290 to ~190 m in the SE Eifel and modified its general shape, namely stretching and straightening its E-W profile (Demoulin and Hallot, 2009). Based on various morphological observations (vertical spacing between river terraces, timing of stream piracy, river sinuosity, geodetic data), the authors also showed that an uplift wave migrated across the massif, starting from its southern margin in the early Pleistocene and currently showing the highest intensity of uplift in the northern Ardennes and Eifel. This recent uplift of the RS occurs within a regional stress field of NW Europe that is primarily determined by the Africa–Eurasia collision and the consequent Alpine push, and the mid-Atlantic ridge push. Since the end of the Miocene, this stress field is characterized by a fan-shaped distribution of $S_{H\max}$ along the northern border of the Alpine arc, giving way to a more consistent N145°E±26° direction of compression farther away from the chain (Bergerat, 1987; Müller et al., 1992).

3. Morphometric indices and uplift age

This study aims to identify geomorphometric variables or to build derived indices that would be sensitive to the time elapsed since a change of the regional base level, induced, e.g., by an en-bloc uplift like that of the WRS during the Quaternary. In order to test various indices, I subdivided the study area into three subareas of distinct uplift age (Demoulin and Hallot, 2009) from north to south, respectively (i) the N Ardennes–N Eifel area, which is still rising currently; (ii) the central Ardennes–S Eifel–N Hunsrück area uplifted in the middle Pleistocene; and (iii) the S Ardennes–S Hunsrück–Saar-Nahe area uplifted in the early Pleistocene (Fig. 1). In each of them, a set of 22 to 35 streams was selected to cover the range of basin size. Because they need to have developed a minimum own tributary network, which one of the basic variables will describe, the smallest streams considered (Strahler order 2) are ~8 km long, with a drainage area of ~15 km^2. The largest rivers of the data set are the Ardennian Ourthe and Sûre (Strahler order 6), with lengths of 145–150 km and drainage areas between 3600 and 4000 km^2.

The time sensitivity of a good indicator should be ensured by its ability to isolate that part of the landscape incision/denudation that responds primarily to the base level signal. A further requirement of valuable variables also is that they can describe, either individually or in combination, specific time-dependent stages of the landscape response on its way toward a new steady state. Under the assumption of a landscape denudation controlled in the first instance by river incision, a relative lowering of the regional base level induces three distinct geomorphic features to react successively: namely firstly the trunk streams, which start to incise rapidly from their outlet upstream toward the interior of the uplifted area; then the drainage network as a whole, in which the wave of regressive erosion progressively propagates; and finally the entire catchments, whose denudation increases at last, following generalized stream incision. Therefore, I attempt to build indices that rely on these three geomorphic features, express them in a comparable standardized way, and may thus be combined in successive complexity levels.

3.1. Elementary indices

The variables used at the elementary level describe each feature individually. At the catchment scale, the hypsometric integral $\int H_b$ appears to be appropriate to describing in a standardized way the long-term response to a base level change. Referring to its expression, I thus propose to describe the short-term response by the similar integral $\int H_r$ of the standardized long profile H_r of the trunk stream of the considered catchment (Fig. 2). Note however that the reference value for standardizing the altitudes of the river profile remains the maximum difference in elevation observed in the catchment, so that the comparison of $\int H_b$ and $\int H_r$ within a given catchment still makes physical sense, notably preserving information about the relative amount of valley incision. As for the middle-term response of the landscape, which is contained in the drainage network of the catchment as a whole, a third integral, $\int H_n$, is computed, referring this time to a 'cumulated long profile' or, better, to an hypsometric curve of the drainage network. Indeed, the H_n curve of Fig. 2

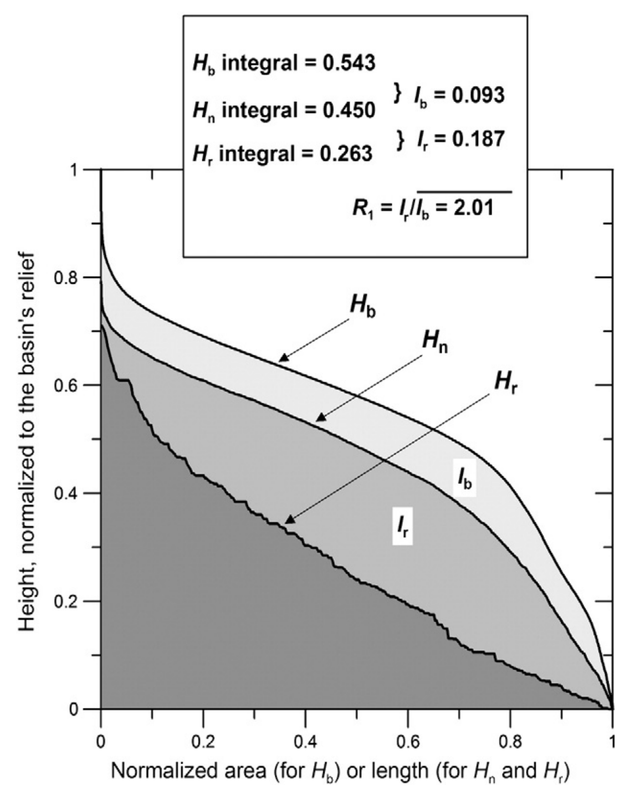

Fig. 2. Description of the indices used to define the index R_1. The diagram refers to the true example of the Ahr River of northern Eifel, with a basin size $A = 896$ km^2. H_b, H_n and H_r denote respectively the basin's hypsometric curve, the drainage network's hypsometric curve and the trunk stream's long profile. I_b (area in light gray) = $\int H_b - \int H_n$ and I_r (area in medium gray) = $\int H_n - \int H_r$.

Please cite this article as: Demoulin, A., Basin and river profile morphometry: A new index with a high potential for relative dating of tectonic uplift, Geomorphology (2010), doi:10.1016/j.geomorph.2010.10.033

Table 1
Indices of the rivers analyzed in the three subareas of the WRS.

	L (km)	A (km^2)	$\int H_b$	$\int H_n$	$\int H_r$	$I_b = \int H_b - \int H_n$	$I_r = \int H_n - \int H_r$	$R_1 = I_r/I_b$	$\int H_n / \int H_b$	$\int H_r / \int H_n$
Area 1										
Ourthe	149.2	3627	0.513	0.440	0.228	0.073	0.212	2.904	0.858	0.518
Vesdre	65.4	704	0.464	0.393	0.260	0.071	0.133	1.873	0.847	0.662
Hoegne	31.2	209	0.456	0.364	0.342	0.092	0.022	0.239	0.798	0.940
Wayai	17.0	100	0.516	0.387	0.258	0.129	0.129	1.000	0.750	0.667
Helle	19.3	70	0.611	0.507	0.423	0.104	0.084	0.808	0.830	0.834
l. Amblève-Holzw.	87.7	1075	0.602	0.512	0.351	0.090	0.161	1.789	0.850	0.686
u. Amblève	27.3	212	0.602	0.475	0.344	0.127	0.131	1.031	0.789	0.724
Salm-B	31.4	236	0.586	0.460	0.341	0.126	0.119	0.944	0.785	0.741
Lienne	26.5	150	0.523	0.396	0.284	0.127	0.112	0.882	0.757	0.717
u. Warche	9.9	30	0.448	0.262	0.217	0.186	0.045	0.242	0.585	0.828
Warchenne	13.4	32	0.655	0.489	0.458	0.166	0.031	0.187	0.747	0.937
Eau Rouge	14.1	50	0.543	0.396	0.364	0.147	0.032	0.218	0.729	0.919
Roannai	10.1	37	0.630	0.380	0.305	0.250	0.075	0.300	0.603	0.803
Eastern Ourthe	32.7	325	0.488	0.388	0.222	0.100	0.166	1.660	0.795	0.572
Aisne	32.0	192	0.490	0.381	0.302	0.109	0.079	0.725	0.778	0.793
Lembrée	15.7	52	0.518	0.381	0.309	0.137	0.072	0.526	0.736	0.811
Lesse	79.7	1338	0.471	0.392	0.224	0.079	0.168	2.127	0.832	0.571
Kall	24.0	76	0.621	0.477	0.402	0.144	0.075	0.521	0.768	0.843
Vicht	25.3	97	0.469	0.372	0.292	0.097	0.080	0.825	0.793	0.785
Rur (Eifel)	69.5	810	0.635	0.529	0.295	0.106	0.234	2.208	0.833	0.558
Urft	42.8	377	0.600	0.475	0.308	0.125	0.167	1.336	0.792	0.648
Olef	28.0	197	0.607	0.451	0.311	0.156	0.140	0.897	0.743	0.690
Wisterbach	11.0	42	0.685	0.513	0.411	0.172	0.102	0.593	0.749	0.801
Perlenbach	15.6	62	0.670	0.521	0.404	0.149	0.117	0.785	0.778	0.775
Ahr	77.7	896	0.543	0.450	0.262	0.093	0.188	2.022	0.829	0.582
Armutsbach	15.2	61	0.601	0.449	0.370	0.152	0.079	0.520	0.747	0.824
Liersbach	13.6	29	0.532	0.355	0.333	0.177	0.022	0.124	0.667	0.938
Sahrbach	15.2	43	0.602	0.412	0.312	0.190	0.100	0.526	0.684	0.757
Area 2										
Sûre	144.9	3987	0.477	0.395	0.212	0.082	0.183	2.232	0.828	0.537
Wark	25.2	82	0.589	0.427	0.279	0.162	0.148	0.914	0.725	0.653
Clerf	42.8	231	0.665	0.533	0.372	0.132	0.161	1.220	0.802	0.698
Wiltz	38.9	439	0.672	0.538	0.363	0.134	0.175	1.306	0.801	0.675
Our	88.3	671	0.551	0.450	0.276	0.101	0.174	1.723	0.817	0.613
Enz	32.6	148	0.609	0.460	0.333	0.149	0.127	0.852	0.755	0.724
Prüm	79.7	887	0.501	0.410	0.296	0.091	0.114	1.253	0.818	0.722
Nims	53.5	283	0.521	0.425	0.310	0.096	0.115	1.198	0.816	0.729
Kyll	114.6	845	0.556	0.468	0.315	0.088	0.153	1.739	0.842	0.673
Salm-D	50.0	294	0.422	0.326	0.273	0.096	0.053	0.552	0.773	0.837
Lieser	58.3	405	0.457	0.367	0.282	0.090	0.085	0.944	0.803	0.768
Kleine Kyll	20.7	87	0.492	0.344	0.258	0.148	0.086	0.581	0.699	0.750
Alf	45.7	358	0.539	0.440	0.332	0.099	0.108	1.091	0.816	0.755
Uess	36.7	184	0.558	0.455	0.370	0.103	0.085	0.825	0.815	0.813
Endertbach	20.3	75	0.650	0.523	0.420	0.127	0.103	0.811	0.805	0.803
Elzbach	44.3	220	0.559	0.468	0.345	0.091	0.123	1.352	0.837	0.737
Dhron	35.9	319	0.513	0.404	0.285	0.109	0.119	1.092	0.788	0.705
kleine Dhron	27.3	137	0.486	0.367	0.266	0.119	0.101	0.849	0.755	0.725
Ruwer	43.8	238	0.542	0.425	0.313	0.117	0.112	0.957	0.784	0.736
Flaumbach	25.5	201	0.655	0.530	0.358	0.125	0.172	1.376	0.809	0.675
Mörsdorfer Bach	16.1	60	0.627	0.490	0.372	0.137	0.118	0.861	0.781	0.759
Alfbach	18.8	56	0.416	0.286	0.212	0.130	0.074	0.569	0.688	0.741
Ulf	11.9	59	0.602	0.405	0.256	0.197	0.149	0.756	0.673	0.632
Heilenbach	12.9	28	0.459	0.325	0.281	0.134	0.044	0.328	0.708	0.865
Simmerbach	49.8	395	0.500	0.410	0.285	0.090	0.125	1.389	0.820	0.695
l. Hahnenbach-Kyrb.	36.6	260	0.426	0.338	0.218	0.088	0.120	1.364	0.793	0.645
u. Hahnenbach	17.6	87	0.413	0.290	0.201	0.123	0.089	0.724	0.702	0.693
Guldenbach	33.2	173	0.529	0.433	0.304	0.096	0.129	1.344	0.819	0.702
l. Lametbach-Brühlb.	15.3	58	0.495	0.345	0.246	0.150	0.099	0.660	0.697	0.713
u. Lametbach	8.0	16	0.619	0.409	0.376	0.210	0.033	0.157	0.661	0.919
Anglier	11.6	30	0.553	0.370	0.269	0.183	0.101	0.552	0.669	0.727
Mellier	18.9	65	0.555	0.400	0.284	0.155	0.116	0.748	0.721	0.710
Vierre	35.6	261	0.454	0.337	0.195	0.117	0.142	1.214	0.742	0.579
r. de Neufchateau	18.5	65	0.468	0.328	0.247	0.140	0.081	0.579	0.701	0.753
Alzette	44.3	895	0.404	0.301	0.102	0.103	0.199	1.932	0.745	0.339
Area 3										
Nahe	116.1	4066	0.361	0.286	0.171	0.075	0.115	1.533	0.792	0.598
Wadrill	22.5	74	0.456	0.336	0.279	0.120	0.057	0.475	0.737	0.830
Idarbach	21.1	94	0.497	0.358	0.270	0.139	0.088	0.633	0.720	0.754
Ellerbach	26.4	186	0.422	0.325	0.239	0.097	0.086	0.887	0.770	0.735
Fischbach	20.4	98	0.428	0.317	0.269	0.111	0.048	0.432	0.741	0.849
Dambach	18.4	64	0.449	0.303	0.255	0.146	0.048	0.329	0.675	0.842
Glan	81.1	1224	0.377	0.273	0.128	0.104	0.145	1.394	0.724	0.469

Please cite this article as: Demoulin, A., Basin and river profile morphometry: A new index with a high potential for relative dating of tectonic uplift, Geomorphology (2010), doi:10.1016/j.geomorph.2010.10.033

Table 1 (*continued*)

	L (km)	A (km^2)	$\int H_b$	$\int H_n$	$\int H_r$	$I_b = \int H_b - \int H_n$	$I_r = \int H_n - \int H_r$	$R_1 = I_r/I_b$	$\int H_n/\int H_b$	$\int H_r/\int H_n$
Area 3										
u. Glan	26.0	198	0.267	0.141	0.083	0.126	0.058	0.460	0.528	0.589
Odenbach	22.9	86	0.576	0.381	0.272	0.195	0.109	0.559	0.661	0.714
Lauterbach	42.3	275	0.318	0.211	0.133	0.107	0.078	0.729	0.664	0.630
Alsenz	49.6	328	0.416	0.294	0.187	0.122	0.107	0.877	0.707	0.636
Grossbach	14.0	42	0.550	0.363	0.298	0.187	0.065	0.348	0.660	0.821
Jeckenbach	19.8	67	0.517	0.356	0.268	0.161	0.088	0.547	0.689	0.753
Moschel	19.6	66	0.468	0.291	0.258	0.177	0.033	0.186	0.622	0.887
Totenalb	15.2	90	0.545	0.382	0.281	0.163	0.101	0.620	0.701	0.736
Ill	32.8	218	0.326	0.205	0.149	0.121	0.056	0.463	0.629	0.727
Kuselbach	16.4	79	0.375	0.246	0.174	0.129	0.072	0.558	0.656	0.707
Oster	27.2	116	0.361	0.211	0.151	0.150	0.060	0.400	0.584	0.716
Bärenbach	11.6	20	0.427	0.290	0.246	0.137	0.044	0.321	0.679	0.848
Alleines	14.2	89	0.641	0.517	0.463	0.124	0.054	0.435	0.807	0.896
Rebais	7.9	14	0.629	0.325	0.274	0.304	0.051	0.168	0.517	0.843
r. de Membre	8.9	17	0.678	0.453	0.374	0.225	0.079	0.351	0.668	0.826

represents the percentage of the network pixels (or cumulated length) whose altitude is higher than a given value (again standardized with respect to the catchment's altitudes). It is assumed to reflect the degree to which an incision wave has propagated from the main stem within the smaller branches of the drainage network.

The three integrals may of course be determined for catchments and nested subcatchments of any size or hierarchical order in a given area. I thus calculated them for all 85 streams of the data set in the WRS and proceeded with the first step of the morphometric analysis, looking for (i) spatial variations of the values of each integral; (ii) correlations between integrals or with other variables such as, e.g., the drainage area A or the length L of the trunk stream; and (iii) regional specificity of the latter.

3.2. Data extraction

Data extraction was carried out with ArcMap, version 9.3.1. The hydrologic correction of the SRTM elevation model was performed using the algorithm of Schaüble (2000) and the first-order streams of the drainage network were defined as starting from a minimum catchment area of ~0.5 km^2. The treatment of a particular river implied firstly the creation of two shapefiles locating respectively its source (hereafter *src_S1*) and outlet (*otl_S1*), then the run of the following script:

```
SnapPourPoint otl_S1 DEM_facc D:\...\g_otl_S1 100
SnapPourPoint src_S1 DEM_facc D:\...\g_src_S1 100
Extent MAXOF
CostDistance g_src_S1 DEM_cost D:\...\S1_costdi
Extent MAXOF
CostBackLink g_src_S1 DEM_cost D:\...\S1_costbl
CostPath g_otl_S1 S1_costdi S1_costbl D:\...\g_S1
ExtractByMask DEM_alti g_S1 D:\...\S1_alti
ExtractByMask S1_costdi g_S1 D:\...\S1_dist
SingleOutputMapAlgebra "int(S1_dist/200) + 1" D:\...\S1_segm
ZonalStatisticsAsTable S1_segm VALUE S1_alti D:\...\S1_profil
Watershed DEM_fdir g_otl_S1 D:\...\S1_bass
ExtractByMask DEM_corr S1_bass D:\...\S1_demb
ExtractByMask DEM_alti S1_bass D:\...\S1_demr
```

where *DEM_corr* is the corrected elevation model, *DEM_fdir* and *DEM_facc* are produced by applying the functions *flow direction* and *flow accumulation*, and *DEM_alti* and *DEM_cost* are two raster files of the drainage network respectively coding pixel altitudes and a fixed value of 1. Finally, the function *TableToTable* is applied to *S1_profil*, *S1_demb* and *S1_demr* to obtain the dbf files used to produce the profiles of the stream, its drainage network and its catchment area. Any ad hoc software (e.g., Grapher of Golden Software) may then be used to calculate the three corresponding integrals.

3.3. Higher level indices

To get closer to the target, the elementary variables may be combined two by two to yield the new variables (Fig. 2):

$$I_b = \int H_b - \int H_n \quad (1)$$

and

$$I_r = \int H_n - \int H_r \quad (2)$$

These two indices, ranging between 0 and 1, aim at comparing the relative evolution of main stem, drainage network, and catchment as revealed by their respective integrals. Briefly said, I_b indicates how much the fluvial system is incised in its catchment, and I_r how far the regressive erosion has invaded the whole drainage network. In general, higher I_r values correspond to a more recent base level change, whereas the temporal evolution of I_b is more complicated (see below). In any case, both I indices may in turn be submitted to the same analysis as the elementary variables.

However, being expressed as differences, they still depend to some extent on the local efficiency of the erosion, i.e., they still contain the lithological parameter that is also implicitly included in the three integrals. Moreover, each I index captures only a part of the complete response process of the catchment. It seems therefore interesting to combine them further within a more comprehensive index that could in principle provide the best relative figure of the time elapsed since a base level change affected a region. Two forms of such a third-level index were tested, the most effective of them, with variations fairly clearly related to their geomorphological causes, being expressed as:

$$R_1 = I_r / I_b = \left(\int H_n - \int H_r\right) / \left(\int H_b - \int H_n\right) \quad (3)$$

Indeed, using ratios should theoretically minimize biases of external origin with respect to the investigated process, i.e., biases that are due to spatial rather than temporal controls (e.g., lithology) and that thus affect the numerator and the denominator in approximately the same way.

Table 2
Mean *m* and standard deviation *s* of the indices, globally and per subarea (*n* = number of rivers).

		$\int H_b$		$\int H_n$		$\int H_r$		I_b		I_r		R_1		$\int H_r/\int H_n$		$\int H_n/\int H_b$	
	n	*m*	*s*	*m*	*s*	*m*	*s*	*m*	*s*	*m*	*s*	*m*	*s*	*m*	*s*	*m*	*s*
Area 1	28	0.56	0.07	0.43	0.06	0.32	0.06	0.13	0.04	0.11	0.06	0.99	0.73	0.75	0.12	0.77	0.07
Area 2	35	0.53	0.08	0.41	0.07	0.29	0.06	0.12	0.03	0.12	0.04	1.03	0.45	0.71	0.10	0.77	0.06
Area 3	22	0.46	0.11	0.31	0.08	0.24	0.09	0.15	0.05	0.08	0.03	0.58	0.34	0.75	0.11	0.68	0.07
WRS	85	0.52	0.09	0.39	0.09	0.29	0.08	0.13	0.04	0.10	0.05	0.90	0.57	0.73	0.11	0.74	0.08

4. Results

Empirical tests have shown that, within the size range of the rivers considered in the study, the error on the calculated indices because of the low resolution of the SRTM 3″ DEM does not affect significantly the results. All $\int H$ indices are biased in the same sense, and approximately with the same amplitude for $\int H_n$ and $\int H_r$, so that the error on the *I* indices is more or less canceled and the error on the R_1 index does not exceed a few percents.

Table 1 presents the data (river length, catchment area, *H* integrals, and the derived indices) for the 85 rivers sampled in the WRS. All analytical results are presented in Tables 2 to 4. Student's *t* tests performed on the regional samples whose means and standard deviations are given in Table 2 have shown that, at the 95% confidence level, no single index (including the ratios $\int H_r/\int H_n$ and $\int H_n/\int H_b$, not mentioned in the previous section) is able to make a complete distinction between all three subareas with different uplift age. This is mostly due to the high intra-group variance. Several indices can, however, isolate the S Ardennes–S Hunsrück–Saar-Nahe area (area 3), which is characterized not only by older uplift but also probably by a lower uplift rate.

As the main feature responsible for intra-group variance seemed to be the varying size of the rivers, the next step of the analysis was to search for correlation between the morphometric indices and a size indicator, namely drainage area *A*. At the same time, possible relationships between the indices were also investigated. Correlation and regression results are displayed in Table 3.

Whereas the linear correlation between the *I* indices, though significant, is rather weak at the WRS level and does not identify the three subareas, the linear relations respectively linking $\int H_b$ to $\int H_n$ and $\int H_n$ to $\int H_r$ are much stronger. Moreover, the latter also has the power of separating the areas of different uplift age. The statistical significance of this regional distinction has been tested in the following manner. The normality of the distribution of the residuals was tested for each regional relation. Then, and although these distributions were mostly non-normal, Hartley's tests of equality of variances were performed, generally leading to the conclusion that nothing could be affirmed regarding such an equality. This authorized a two-step comparison of the regressions to be carried out by an Ancova analysis, first testing the equality of the regressions, then, were they different, their parallelism (Sokal and Rohlf, 1981; Dagnelie, 2006) (Table 4). In the case of $\int H_n = f(\int H_r)$, the regional functions are significantly different but statistically parallel, indicating that the regional (uplift age) variable controls $\int H_n$ independently of $\int H_r$ (and vice-versa).

As for the correlations with basin area *A*, they all take a logarithmic form. At the WRS level, $\int H_b$ and $\int H_r$ display only weak correlation to ln*A*, and $\int H_n$ shows no correlation at all. By contrast, the *I* indices, R_1, and another ratio, $\int H_r/\int H_n$, are tightly linked to ln*A*. The regressions on ln*A* of two of them, namely I_r and R_1, are moreover regionally different and nonparallel. The test values for the regional differentiation of $R_1 = f(\ln A)$ show that this relation is by far the most discriminating (Fig. 3). It will thus be treated hereafter as the best reference for uplift age and discussed by means of a further index corresponding to its regression slope S_r (equivalent to the parameter a of the relation in Table 3).

Another issue of the study was to decide whether the morphometric indices and relations are more realistically obtained from their evolution along a single stream representative of the investigated area or from a large set of rivers, as exposed until here. Three main rivers have thus been chosen, namely the Ourthe in area 1, the Sûre in area 2, and the Nahe in area 3 (Fig. 1) and the R_1 index has been calculated at regular intervals along their course, deriving each time the indices from upstream profiles ending down at the considered point of the river. The resulting curves are compared in Fig. 4 with those yielded by the river sets. In areas 1 and 2, the similarity between the curves of, respectively, the Ourthe or the Sûre and the corresponding regional river set is remarkable. Not only are the curves almost superposed, with S_r index values almost identical, but the correlations with ln*A* are even better for the main river data (moreover relying on higher *n*: *n* (Ourthe) = 45, *n*(Sûre) = 44) than for the river sets. However, unlike the quite uniform curve of the Ourthe, the Sûre curve shows a marked local irregularity located at the confluence with a major tributary, the Alzette, which drains a region (22% of the Sûre whole catchment) that does not pertain to area 2 but to area 3 (Fig. 1). A similar but higher amplitude perturbation also affects the curve of the Nahe, again reflecting the heterogeneity of the catchment. Indeed, before the Nahe receives its main tributary, the Glan, and takes its character typical of area 3, its upper and middle course drains a part of the Hunsrück that pertains to area 2 for ~40% of the whole catchment of the river (Fig. 1).

Table 3
Linear correlation '$Y = a*X + b$' between various variables (*n* = number of rivers; *ρ* = Pearson's coefficient of correlation); the correlations that display regional differentiation (see Table 4) are in bold; no parameter is calculated for correlations nonsignificant at the 95% confidence level.

		Area 1 (*n* = 28)			Area 2 (*n* = 35)			Area 3 (*n* = 22)			WRS (*n* = 85)		
X	*Y*	*ρ*	*a*	*b*	*ρ*	*a*	*b*	*ρ*	*a*	*b*	*ρ*	*a*	*b*
$\int H_n$	$\int H_b$	0.81	0.90	0.17	0.91	0.99	0.13	0.91	1.19	0.09	0.90	0.98	0.14
$\int H_r$	**$\int H_n$**	**0.61**	**0.60**	**0.24**	**0.84**	**0.91**	**0.14**	**0.95**	**0.92**	**0.09**	**0.84**	**0.94**	**0.12**
I_r	I_b	0.51	−0.37	0.17	0.25	–	–	0.25	–	–	0.40	−0.35	0.17
ln*A*	$\int H_b$	0.27	–	–	0.17	–	–	0.62	−0.05	0.71	0.26	−0.02	0.62
ln*A*	$\int H_n$	0.22	–	–	0.17	–	–	0.38	−0.02	0.43	0.09	–	–
ln*A*	$\int H_r$	0.50	−0.02	0.44	0.19	–	–	0.57	−0.04	0.42	0.32	−0.02	0.39
ln*A*	I_b	0.79	−0.03	0.26	0.79	−0.02	0.24	0.73	−0.03	0.28	0.77	−0.03	0.26
ln*A*	**I_r**	**0.82**	**0.04**	**−0.07**	**0.63**	**0.02**	**0.01**	**0.62**	**0.01**	**0.01**	**0.69**	**0.03**	**−0.03**
ln*A*	**R_1**	**0.93**	**0.51**	**−1.59**	**0.88**	**0.35**	**−0.77**	**0.89**	**0.24**	**−0.54**	**0.87**	**0.39**	**−1.07**
ln*A*	$\int H_r/\int H_n$	0.82	−0.07	1.12	0.57	−0.05	0.96	0.78	−0.07	1.06	0.72	−0.06	1.05

Please cite this article as: Demoulin, A., Basin and river profile morphometry: A new index with a high potential for relative dating of tectonic uplift, Geomorphology (2010), doi:10.1016/j.geomorph.2010.10.033

Table 4
Tests of equality (F_{calc1}) and of parallelism (F_{calc2}) of regional regressions for various relations[a].

Relation	F_{calc1}	F(0.95;4;79) (Snedecor)	F_{calc2}	F(0.95;2;79) (Snedecor)
$\int H_b = f(\int H_n)$	2.10	2.49	–	–
$\int H_n = f(\int H_r)$	**6.58**	**2.49**	2.52	3.11
$I_b = f(\ln A)$	0.90	2.49	–	–
$\boldsymbol{I_r = f(\ln A)}$	**6.80**	**2.49**	**5.41**	**3.11**
$\boldsymbol{R_1 = f(\ln A)}$	**14.62**	**2.49**	**16.13**	**3.11**
$\int H_r / \int H_n = f(\ln A)$	[illegible]	2.49	–	–

$F_{calc1} = \frac{\Delta SSR / 2(p-1)}{\sum_{i=2}^{p}(SSR)_i / (n-2p)}$ with $\Delta SSR = \sum_{i=1}^{p}(SSR)_i - SSR$; SSR = sum of squared residuals of the whole dataset; p = number of groups; n = total number of values.

$F_{calc2} = \frac{\Delta SSR\| / (p-1)}{\sum_{i=2}^{p}(SSR\|)_i / (n-2p)}$ with $\Delta SSR\| = \sum_{i=2}^{p}(SSR\|)_i - SSR$ and $(SSR\|)_i$ = sum of squared residuals for the ith group adjusted with a regression coefficient corresponding to the weighted average of those of all groups.

[a] The values in bold indicate the relations that do not satisfy the null hypothesis and are thus statistically different between the subareas of different uplift age.

Consequently, the S_r index value of the upper/middle Nahe conforms with that of area 2, whereas the curve of the lower Nahe is fairly superimposed on that of area 3, despite its different S_r value (note however that the whole Nahe has the same S_r as area 3). Therefore, in order to prevent such pitfalls in the data interpretation, it seems generally preferable to rely on a large set of rivers to characterize a particular area.

5. Discussion

5.1. Varying mixing of several effects on the morphometric indices

The results indicate that no direct morphometric variable has the power of distinguishing between areas uplifted at different times and that only some relations between variables display a regional (i.e., uplift age-dependent) character. This results from the interplay of a number of factors influencing the relative response rates of the various morphological components within a catchment undergoing tectonic uplift. Beyond uplift age, which is tested here, such factors as climate, lithology, uplift rate, basin size, spatial scale (see later discussions), basin heterogeneity, and anomalous basin shape may determine the landscape's morphological evolution and thus the values taken at a given time by morphometric indices. In the study area, climate may however be put aside as no significant climatic contrast is observed across the WRS. As for the basin lithological or morphological heterogeneity, the Sûre and Nahe cases showed that the morphometric indices of a heterogeneous catchment are very close to those of the region to which its main part pertains. Basins whose anomalous shape biases the morphometric indices were easily identified and removed from the dataset because their index values belonged systematically to the largest outliers. In these cases, the decisive shape characteristic seemed to be the unbalanced distribution of tributaries along the main stream, which induces a lateral shift between the H_n and H_r curves (Fig. 5).

Let's consider now the remaining influences on the various indices presented. The three $\int H$ indices display no regional effect, varying quasi-randomly throughout the whole study area. Lithology and bedrock erodibility certainly play a major role in their variations and explain also the general correlations between the $\int H$ types (Table 3). Basin size exerts only a secondary influence on them. As shown by weak to moderate correlations with $\ln A$ (Table 3), this influence is stronger on $\int H_r$, which provides the fastest response to any base level change, and especially in area 3, whose older uplift left more time for the response at the various morphological levels to adjust to drainage area. Incidentally, note that the use of relative altitude and area in the hypsometric integral $\int H_b$ is often supposed to free it from drainage basin size (Pérez-Peña et al., 2010). The same should thus be true for $\int H_n$ and $\int H_r$, which are constructed the same way. However, this study and others (Hurtrez et al., 1999; Chen et al., 2003) demonstrated some dependence of such integrals on A (inverse correlation). This probably refers to the way erosion propagates with time in the drainage network, by upstream migration of knickpoint from the streams and river reaches of larger A toward those of smaller A. In this sense, the $\int H$ integrals are indeed normalized with respect to space, but not with respect to time, and they should show dependence on A in areas where the morphological component to which they correspond is currently adjusting.

The I indices are only differences of two $\int H$ and, as such, still contain direct information about erosion amount and thus also about lithological control that still masks any possible regional differentiation. However, as a result of the partial cancelation of the lithological effect by differencing, they display a much better overall correlation with $\ln A$ than any $\int H$. The positive correlation between I_r and $\ln A$ indicates that the trunk stream incision is all the more ahead of that of its drainage network as the basin size increases. By contrast, the slightly negative correlation between I_b and $\ln A$ (which is improved in the form of a power law: $I_b = 0.58 * (\ln A)^{-0.97}$; $\rho = 0.84$; $n = 85$) is less well explained, seeming to be basically a scale effect. For greater A associated with a lower base level and a greater relief of the basin, the portion of the hydrographic network with altitudes close to that of the catchment's base level decreases so that, starting from the right of the graph of Fig. 2, the H_n curve tends to diverge faster from H_r, to come closer to H_b and to run parallel with it, leading to smaller I_b.

As for the regional differentiation of the relation $I_r = f(\ln A)$, it indicates that, once the basin size effect is accounted for, the dependence of I_r on the uplift age is high enough to predominate over the remaining noise of lithological origin. The same happens for the relation $\int H_n = f(\int H_r)$: as the lithological noise affects both members of the equation in approximately the same way, it is more or less canceled, allowing the temporal effect (i.e., uplift age) to come out. Moreover, in this case, the parallelism of the three regression lines (Table 4) underlines that the effect of uplift age on H_n and H_r is formally separated from that of other variables (e.g., lithology).

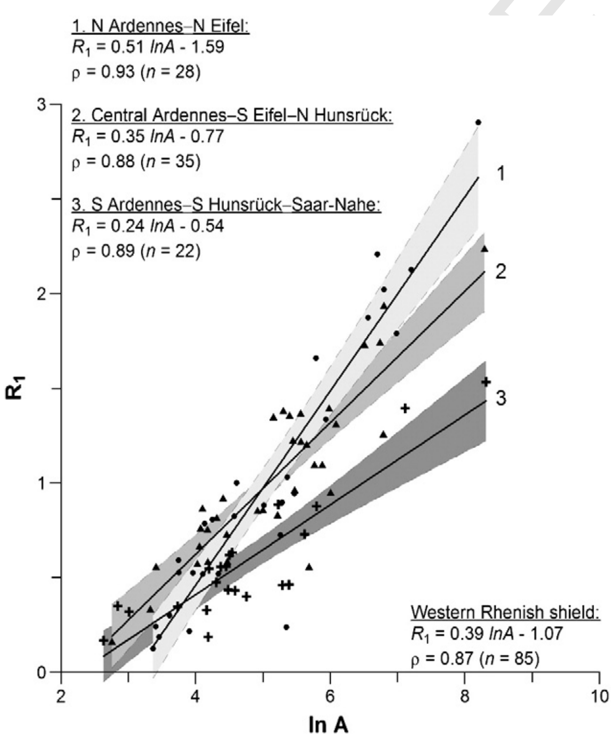

Fig. 3. Correlation of the index R_1 with the logarithm of basin size in the three areas of different uplift age in the WRS (in gray: 95% confidence bands). Solid circles denote rivers of area 1, triangles are for rivers of area 2, and crosses for rivers of area 3.

Please cite this article as: Demoulin, A., Basin and river profile morphometry: A new index with a high potential for relative dating of tectonic uplift, Geomorphology (2010), doi:10.1016/j.geomorph.2010.10.033

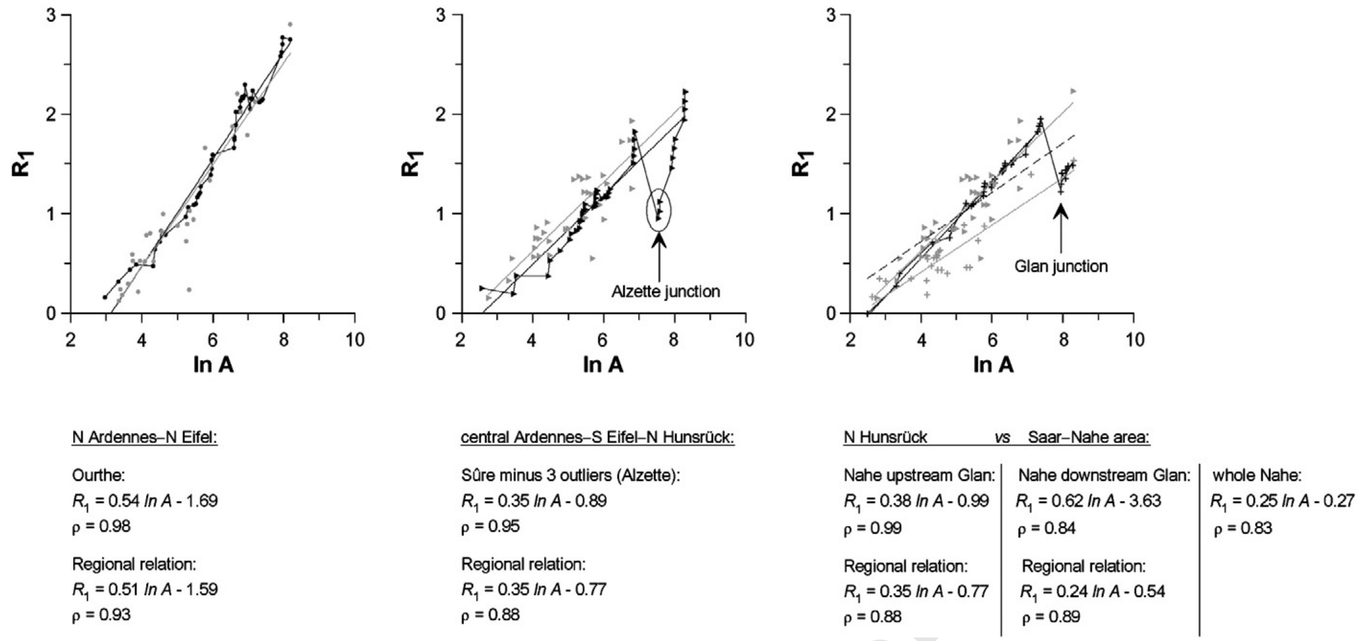

Fig. 4. Comparison in each area of two regression lines $R_1 = f(\ln A)$ based respectively on the evolution along a single representative river (black lines and symbols) and on the whole set of rivers of the area (gray lines and symbols). The relations obtained are compared below, showing that single river analysis yields better correlations but may contain confusing features resulting from the catchment heterogeneity.

However, some residual perturbation persists in both cases, either from lithology on the former relation or from basin size on the latter. These obstacles to an unambiguous evidencing of the regional uplift age effect are surmounted by the relation $R_1 = f(\ln A)$. Indeed, on one hand, the link between R_1 and basin size is much narrower than that between $\ln A$ and any other index (Table 3), thus modeling and removal of the size influence are more efficient; and on the other hand, it was already stressed that the formulation of R_1 as a ratio is best adapted to cancel spatial effects such as lithology. Therefore, the remaining variations of R_1, expressed through the S_r index, are amply dominated by the temporal effect and S_r unquestionably provides the most robust information about uplift age.

To this point, there are however still two restrictions to the conclusion that the S_r index value is actually revealing the relative age of regional uplift. The first is that another variable, namely uplift rate, has not yet been involved in the discussion, though it might as well have a regional character. Indeed, the two variables, uplift age and rate, remain difficult to separate on the basis of morphological indices, this all the more as they really may be geo-dynamically linked. In the WRS study area, the S Ardennes–S Hunsrück–Saar-Nahe region (area 3) is characterized not only by particular values of the morphological indices but also by a mean altitude lower than in the other subareas. This suggests that uplift age and rate may both contribute to determine the parameters of its relation $R_1 = f(\ln A)$, but it is not clear whether uplift rate interferes with uplift age in fixing the value of S_r or rather explains the apparently very low b value of the equation. The fact that there is no significant difference in altitude between areas 1 and 2 might indicate that uplift rate and amount were similar and therefore that the main influence on S_r is uplift age. Unfortunately, spatial and especially N–S variations in Quaternary uplift rate in the WRS are too poorly documented for a deeper investigation of this issue, which obviously deserves a specific analysis in a region where variations in uplift rate (or amount) predominate over timing (though intermingling of both influences is just what renders the problem complex).

The second provisional restriction refers to the geomorphological consistency of the interpretation made of the relation between R_1, basin size, and time. The next section examines whether the way R_1 and S_r evolve with time may be theoretically predicted and which role basin size is expected to play in this frame.

5.2. Theoretical meaning of the R_1 and S_r indices

Gradients in the upstream reaches of rivers of the WRS are almost always below 5%, i.e., in the range where Hovius (2000) showed that the interplay between various external controls (uplift rate, rainfall amount, lithology, etc.) causes considerable scatter in mean river long profile between regions. Simple indices derived from such profiles thus struggle to isolate a particular effect. However, in these rivers, removal of the material provided by upstream erosion and bedrock incision is thought to occur primarily by knickpoint migration (e.g., Seidl and Dietrich, 1992; Whipple and Tucker, 1999) and this is the key to the effectiveness of R_1 and S_r to capture time information within the transient response to a base level change.

Assume a region at steady state suddenly affected by a base level lowering, corresponding either to en-bloc uplift of a main catchment or, at a nested scale, to the arrival of a retreating knickpoint at the outlet of a tributary catchment (Fig. 6). Obviously, this base level change, which causes an 'instantaneous' similar increase of all $\int H$ but no immediate variation of R_1, induces firstly incision of the trunk stream, where the knickpoint propagates fastest, in power law relation with basin size (knickpoint celerity $c_{KP} \propto A^m$, with $m > 0$, see, e.g., Whipple and Tucker, 1999). Therefore, the initial response of the system is characterized by a marked decrease of $\int H_r$, while $\int H_n$ diminishes only slightly and $\int H_b$ hardly changes, leading to I_r increasing much more than I_b, and consequently R_1 getting rapidly higher. In the middle-term ($>10^5$ years), however, the knickpoint migrates at progressively slower speed in the upper course of the trunk, while incision propagates simultaneously in an increasing number of tributaries and sub-tributaries so that the decrease of $\int H_r$ slows down and, concurrently, that of $\int H_n$ accelerates strongly. In the same time, $\int H_b$ is still more or less unaffected. This stage of the evolution, lasting probably a few million years in areas of moderate uplift and relief like the WRS, thus opposes a gradually decreasing I_r to an increasing I_b, resulting in a decrease of R_1 with time. In the long-term ($>10^6$ years), the drainage network finally reaches a new state of dynamic equilibrium and the

Please cite this article as: Demoulin, A., Basin and river profile morphometry: A new index with a high potential for relative dating of tectonic uplift, Geomorphology (2010), doi:10.1016/j.geomorph.2010.10.033

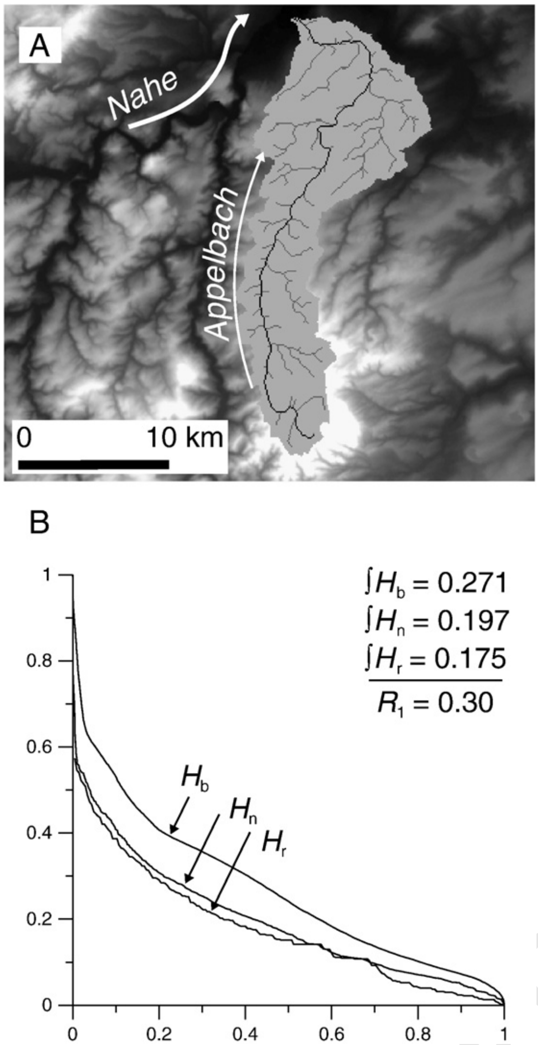

Fig. 5. Influence of the basin shape on the morphometric indices. (A) Map of the Appelbach catchment (tributary of the Nahe, area 3). (B) Corresponding H curves and R_1 index. In this case, not only does the irregular shape of the catchment, with more than half the total tributary length in its lowest fourth part, cause H_n to be very close to H_r, but also the contrast between the largest part of the catchment at comparatively low altitudes and its source located on a summit more than 200 m higher than its immediate surroundings makes H_b anomalously low too.

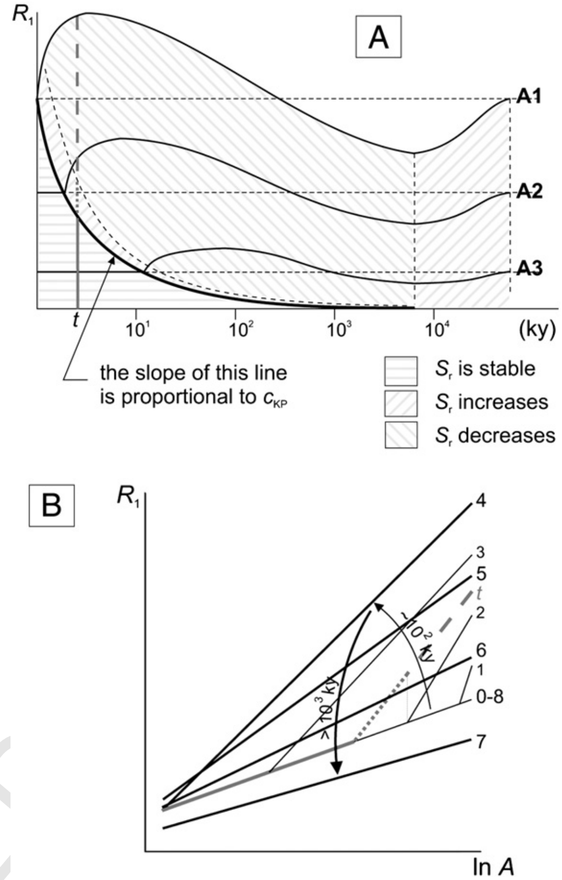

Fig. 7. (A) Evolution of R_1 in function of time for different catchment sizes (A1>A2>A3). The starting time of R_1 change is all the more delayed as one considers smaller tributary catchments, in inverse proportion with the decreasing celerity of the erosion wave migration. (B) Change with time of the curve $R_1 = f(\ln A)$. After a comparatively brief (10^0–10^2 ky) initial increase of the slope S_r shifting gradually from the right to the left of the curve (stages 0 to 4), the latter flattens again over the longer term (>10^3 ky) when erosion is active within the whole drainage network (stages 4 to 7). Finally, a slight reincrease of S_r occurs when the drainage network is at equilibrium and interfluve denudation predominates (stage 8). The curve at time t refers at a particular moment located in Fig. 7A and shows the basin size domains concomitantly experiencing stability, increase, or decrease of S_r (with respect to the preceding stage 2).

signal is fully transmitted to the interfluves: $\int H_b$ turns decreasingly significant whereas $\int H_n$ and $\int H_r$ are now stable: I_b diminishes for I_r constant and R_1 starts therefore to reincrease slowly.

In this scheme, the starting time, the rate, and the amplitude of the R_1 variations are of course catchment size-dependent. Fig. 7A conceptually describes the R_1 evolution with time for three catchments of different sizes. As the erosion wave needs time to propagate toward smaller catchments, the average lag of the latter's evolution

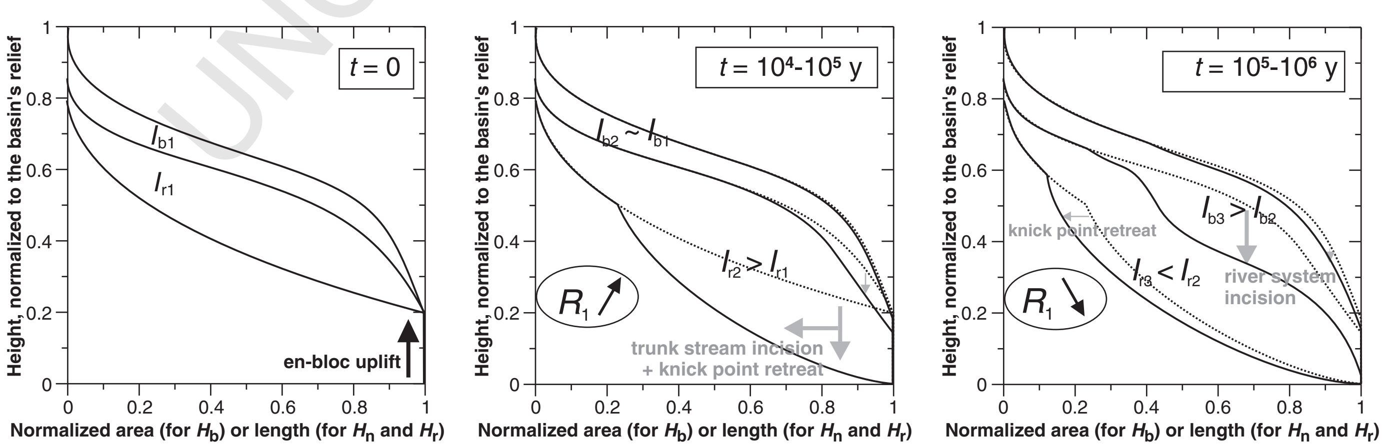

Fig. 6. Conceptual sketches of the successive responses of H_r, H_n, and H_b to a pulse of en-bloc uplift, and implications for the ratio R_1 via the changes in I_r and I_b.

Please cite this article as: Demoulin, A., Basin and river profile morphometry: A new index with a high potential for relative dating of tectonic uplift, Geomorphology (2010), doi:10.1016/j.geomorph.2010.10.033

increases as an inverse power law of their size (i.e., in inverse proportion with the decreasing celerity of the erosion wave). From the comparison of the R_1(A1) and R_1(A2) curves of Fig. 7A, with A1 > A2, it is clear that there is firstly a rapid increase of S_r (indicated by the increasing vertical spacing between the two curves) in the [A1, A2] range, followed by a slow decline of the index that starts when the incision enters the tributary A2 basin while the R_1 increase has already slowed down in the A1 basin (as the interfluve denudation is governed by other processes and takes much more time than river incision, the reincrease of S_r from $\int H_b$ decrease will occur much later). However, toward the headwaters, the response time lag continues to grow for smaller and smaller basins so that there is also a time lag in the change of S_r: the slope of the left part (smaller basins) of the $R_1 = f(\ln A)$ curve remains unchanged for a while before starting to evolve (Fig. 7B). Transposing the observations made between A1, A2, and A3 to infinitely small successive [A, A + ε] intervals, one obtains that the initial phase of rapid S_r increase concerns first the right part (larger basins) of the $R_1 = f(\ln A)$ curve and, operating at any time over a narrow range of A, is progressively shifted toward the smaller basins domain. Based on data compiled in the knickpoint celerity — drainage area diagram of Loget and Van den Driessche (2009), this right-to-left shift of the S_r increase phase (Fig. 7B, stages 0 to 4) is estimated to cover the meaningful part of the $R_1 = f(\ln A)$ curve, i.e., the part above $\ln A \approx 5$, or $A \approx 150$ km^2 (Fig. 3), within a maximum 10^5 years. However, as the response of the main rivers in an uplifted area is very rapid (in the order of 10^4 years) with respect to the subsequent evolution of the rest of their catchments, one may admit that, for these rivers, the morphometric analysis will generally overlook the short-term increase in R_1 and mainly capture its continuous middle-term decrease, which will thus provide unambiguous information about relative uplift ages (Fig. 7). Therefore, although river incision and the R_1 evolution basically start with the uplift, it will often be that, in the case of a short-lived uplift pulse, the initial phase of R_1 and S_r increase is completed for a large range of basin sizes when the pulse ends and that the decrease of both indices (Fig. 7B, stages 4 to 7) thus marks the time passed since that moment.

The results of the morphometric analysis in the WRS, notably the observed spatial variations of S_r, are perfectly consistent with these theoretical developments about the $S_r = f(t)$ relation. Indeed, the most recently uplifted area 1 displays the highest S_r value while area 2, centered on the Mosel valley and affected by an uplift pulse around 0.8 Ma, displays an intermediate value and the southernmost S Ardennes–S Hunsrück–Saar-Nahe area, whose uplift peaked before 1 Ma, has the lowest value. The regional variations of the relation $R_1 = f(\ln A)$, expressed by means of the S_r index, seem therefore to really have this particular geomorphological meaning that they depend mainly on the uplift age.

6. Conclusion

Taking the WRS as a test case, I have developed a morphometric analysis aimed at evaluating the relative timing of regional uplift and based on the combined use of indices describing the successive geomorphic levels at which a catchment responds to a base level change. The newly defined elementary indices $\int H$ extend the concept of the hypsometric integral to the drainage network and to individual river long profiles. The useful final index $R_1 = (\int H_n - \int H_r)/(\int H_b - \int H_n)$ showed no direct relation with the varying uplift age of the three subareas identified in the WRS because it is mainly correlated to the drainage area. However, this correlation is so high that the removal of the modeled drainage area effect does not bias the residuals, from which other influences on R_1 may thus easily be recognized. Among them, the influence of lithology was minimized by expressing the R_1 index as a ratio. It has then been shown that the chief remaining effect seems to be that of uplift age, which is estimated, in relative terms, by the value of S_r, the slope of the relation $R_1 = f(\ln A)$. Indeed, in the WRS case, the variation of S_r with time as deduced from its changes between the subareas fully agrees with its theoretical evolution. The S_r index appears therefore as a particularly promising indicator of the relative timing of a base level change. Describing the transient response to the latter, a quantified relation $S_r = f(t)$ has however still to be searched for. We currently know that $S_r \propto 1/t$, but further research, and especially the estimation of S_r in many other areas of known uplift age and in regions with more rapid tectonic processes, are needed to confirm the relation, to give it a mathematical form, and perhaps, to parameterize it and tend toward (semi-) quantitative age estimates.

Appendix A. Supplementary data

Supplementary data to this article can be found online at doi:10.1016/j.geomorph.2010.10.033.

References

Bergerat, F., 1987;. Stress fields in the European platform at the time of Africa-Eurasian collision. Tectonics 6, 99–132.

Boenigk, W., Frechen, M., 2006;. The Pliocene and Quaternary fluvial archives of the Rhine system. Quaternary Science Reviews 25, 550–574.

Bull, W., McFadden, L., 1977. Tectonic Geomorphology North and South of the Garlock Fault, California. In: Doehring, D. (Ed.), Geomorphology in Arid Regions. Proceedings 8th Annual Geomorphology Symposium, pp. 115–137. Binghamton, NY.

Chen, Y., Sung, Q., Cheng, K., 2003. Along-strike variations of morphotectonic features in the western foothills of Taiwan: tectonic implications based on stream-gradient and hypsometric analysis. Geomorphology 56, 109–137.

Cohen, S., Willgoose, G., Hancock, G., 2008. A methodology for calculating the spatial distribution of the area-slope equation and the hypsometric integral within a catchment. Journal of Geophysical Research 113, F03027. doi:10.1029/2007JF000820.

Dagnelie, P., 2006. Statistique théorique et appliqué. Tome 2. Inférence statistique à une et à deux dimensions. De Boeck et Larcier, Brussels, Belgium. 734 p.

Delcaillau, B., Deffontaines, B., Angelier, J., Déramond, J., Floissac, L., Souquet, P., Chu, H., 1998. Morphotectonic evidence from lateral propagation of an active frontal fold, the Pakuashan anticline: foothills of Taiwan. Geomorphology 24, 263–290.

Demoulin, A., 1998. Testing the tectonic significance of some parameters of longitudinal river profiles: the case of the Ardenne (Belgium, NW Europe). Geomorphology 24, 189–208.

Demoulin, A., Hallot, E., 2009. Shape and amount of the Quaternary uplift of the western Rhenish shield and the Ardennes (western Europe). Tectonophysics 474, 696–708.

Demoulin, A., Hallot, E., Rixhon, G., 2009. Amount and controls of the Quaternary denudation in the Ardennes massif (western Europe). Earth Surface Processes and Landforms 34, 1487–1496.

Goldrick, G., Bishop, P., 2007. Regional analysis of bedrock stream long profiles: evaluation of Hack's SL form, and formulation and assessment of an alternative (the DS form). Earth Surface Processes and Landforms 32, 649–671.

Hack, J., 1957. Studies of longitudinal stream profiles in Virginia and Maryland. Professional Paper 294-B U.S. Geological Survey, pp. 45–97.

Hack, J., 1973. Stream-profile analysis and stream-gradient index. Journal of Research of the U.S. Geological Survey 1, 421–429.

Harlin, J., 1978. Statistical moments of the hypsometric curve and its density function. Mathematical Geology 10, 59–72.

Hovius, N., 2000. Macroscale Process Systems of Mountain Belt Erosion. In: Summerfield, M. (Ed.), Geomorphology and Global Tectonics. Wiley, Chichester, UK, pp. 77–105.

Hurtrez, J., Lucazeau, F., 1999. Lithological control on relief and hypsometry in the Hérault drainage basin (France). Comptes Rendus Académie des Sciences. Earth and Planetary Sciences 328, 687–694.

Hurtrez, J., Sol, C., Lucazeau, F., 1999. Effect of drainage area on hypsometry from an analysis of small-scale drainage basins in the Siwalik Hills (central Nepal). Earth Surface Processes and Landforms 24, 799–808.

Lifton, N., Chase, C., 1992. Tectonic, climatic and lithologic influences on landscape fractal dimension and hypsometry, implications for landscape evolution in the San Gabriel Mountains, California. Geomorphology 5, 77–114.

Loget, N., Van den Driessche, J., 2009. Wave train model for knickpoint migration. Geomorphology 106, 376–382.

Merritts, D., Hesterberg, T., 1994. Stream networks and long-term surface uplift in the New Madrid seismic zone. Science 265, 1081–1084.

Merritts, D., Vincent, K., 1989. Geomorphic response of coastal streams to low, intermediate and high rates of uplift, Mendocino triple junction region, northern California. Geological Society of America Bulletin 101, 1373–1388.

Müller, B., Zoback, M.L., Fuchs, K., Mastin, L., Gregersen, S., Pavoni, N., Stephansson, O., Ljunggren, C., 1992. Regional patterns of tectonic stress in Europe. Journal of Geophysical Research 97/B, 11783–11803.

Pérez-Peña, J., Azañón, J., Booth-Rea, G., Azor, A., Delgado, J., 2009. Differentiating geology and tectonics using a spatial autocorrelation technique for the hypsometric integral. Journal of Geophysical Research 114, F02018. doi:10.1029/2008JF001092.

Please cite this article as: Demoulin, A., Basin and river profile morphometry: A new index with a high potential for relative dating of tectonic uplift, Geomorphology (2010), doi:10.1016/j.geomorph.2010.10.033

Pérez-Peña, J., Azor, A., Azañón, J., Keller, E., 2010. Active tectonics in the Sierra Nevada (Betic Cordillera, SE Spain): insights from geomorphic indexes and drainage pattern analysis. Geomorphology 119, 74–87.

Schaüble, H., 2000. Erosionsmodellierungen mit GIS. Probleme und Lösungen zur exakten Prognose von Erosion und Akkumulation. GIS in der Geographie. II. Ergebnisse der Jahrestagung des Arbeitskreises GIS 25/26, Univ. Tübingen 51–62.

Seidl, M., Dietrich, W., 1992. The problem of channel erosion into bedrock. Catena supplement 23, 101–124.

Sokal, R., Rohlf, J., 1981. Biometry: the principles and practice of statistics in biological research. Freeman and Company, San Francisco. 859 p.

Sougnez, N., Vanacker, V., 2009. Spatial variability in channel and slope morphology within the Ardennes Massif, and its link with tectonics. Proceedings of Geomorphometry 2009, Zurich. http,//www.geomorphometry.org/system/files/sougnez2009geomorphometry.pdf.

Strahler, A., 1952. Hypsometric (area–altitude curve) analysis of erosional topography. Geological Society of America Bulletin 63, 1117–1141.

Strahler, A., 1957. Quantitative analysis of watershed geomorphology. Transactions of the American Geophysical Union 38, 913–920.

Van Balen, R., Houtgast, R., Van der Wateren, F., Vandenberghe, J., Bogaart, P., 2000. Sediment budget and tectonic evolution of the Meuse catchment in the Ardennes and the Roer Valley Rift System. Global and Planetary Change 27, 113–129.

Van den Berg, M., 1996. Fluvial sequences of the Maas. A 10 Ma record of neotectonics and climate change at various time-scales. PhD, Landbouwuniversiteit Wageningen, 181 p.

Walcott, R., Summerfield, M., 2008. Scale dependence of hypsometric integrals: an analysis of southeast African basins. Geomorphology 96, 174–186.

Whipple, K., Tucker, G., 1999. Dynamics of the stream power river incision model: implications for height limits of mountain ranges, landscape response timescales and research needs. Journal of Geophysical Research 104/B, 17661–17674.

Willgoose, G., 1994. A physical explanation for an observed area–slope–elevation relationship for catchments with declining relief. Water Resources Research 30, 151–159.

Ziegler, P., Dèzes, P., 2007. Cenozoic uplift of Variscan massifs in the Alpine foreland: timing and controlling mechanisms. Global and Planetary Change 58, 237–269.

Please cite this article as: Demoulin, A., Basin and river profile morphometry: A new index with a high potential for relative dating of tectonic uplift, Geomorphology (2010), doi:10.1016/j.geomorph.2010.10.033